Theor Chim Acta (1987) 72: 1-12

Theoretica Chimica Acta

Converged calculations of vibrational energy transfer probabilities for the collision of two HF($v = 1$) molecules

David W. Schwenke and Donald G. Truhlar

Department of Chemistry and Supercomputer Institute, University of Minnesota, Minneapolis, MN 55455, USA

(Received February 2/Accepted March 31, 1987)

We present converged quantum mechanical calculations of state-to-state transition probabilities for the collision of two hydrogen fluoride molecules with zero total angular momentum. The potential energy surface is obtained by adding a vibrational dependence to the interaction potential of Alexander and DePristo. We have calculated converged transition probabilities for vibration-to-vibration and vibration-to-translation-and-rotation energy transfer including full vibration-rotation coupling. The calculations include up to 948 coupled channels. Final production runs were carried out with a highly vectorized code on the Minnesota Supercomputer Institute's Control Data Corporation Cyber 205 computer.

Key words: Scattering — Collision dynamics — Close coupling — Vibrational energy transfer — Pipeline vector computer

1. Introduction

Vibration-to-vibration(V-V) energy transfer is usually much faster than vibration-to-translation (V-T) or vibration-to-rotation (V-R) energy transfer, and hence it plays a central role in molecular energy relaxation under many circumstances [1, 2]. Rigorous treatments have lagged behind those for other forms of energy transfer though because V-T and V-R processes occur in atom-diatom collisions, but V-V processes only occur in atom-triatom, diatom-diatom, or larger systems, and the extra degrees of freedom make a converged quantal solution very difficult. We have begun a large-scale computational effort directed

to this problem, and in the present article we report a converged solution to the nuclear-motion Schroedinger equation for collisions of two HF molecules with a very approximate potential energy surface and with the total angular momentum zero. We are encouraged by this success, and we hope in future work to obtain converged solutions for a more accurate potential energy surface and for nonzero total angular momenta, both of which would be required to compare our results to experiment.

The potential energy surface used for this work is called the modified Alexander-DePristo (MAD) surface, and is described below. The method used for the dynamics calculations is R matrix propagation. Our implementation and vectorization of this algorithm for three-dimensional diatom-diatom collisions is described in detail in a previous paper [3] and is only summarized briefly here. Preliminary results for V-V transition probabilities were reported in a Communication in this journal [4] and a conference paper [5]; final results are reported here and are compared to the calculated transition probabilities for vibration-to-translation-and-rotation (V-T, R) energy transfer.[1]

2. Potential energy function

We begin with the HF-HF interaction potential of Alexander and DePristo [6], which is a fit to the *ab initio* SCF data of Yarkony et al [7]. This potential is defined for both diatoms at their equilibrium separations, and it is given by

$$\mathcal{V} = (4\pi)^{3/2} \sum_{\lambda_1\lambda_2\lambda} U^e_{\lambda_1\lambda_2\lambda}(r)\, Y_{\lambda_1\lambda_2\lambda}(\hat{\boldsymbol{r}}, \hat{\boldsymbol{R}}_1, \hat{\boldsymbol{R}}_2), \tag{1}$$

where

$$Y_{\lambda_1\lambda_2\lambda} = \sum_{m_1 m_2 m} (\lambda_1 m_1 \lambda_2 m_2 | \lambda_1 \lambda_2 \lambda m)\, Y_{\lambda_1 m_1}(\hat{\boldsymbol{R}}_1)\, Y_{\lambda_2 m_2}(\hat{\boldsymbol{R}}_2)\, Y^*_{\lambda m}(\hat{\boldsymbol{r}}), \tag{2}$$

where r is the distance between the centres of mass of the two molecules, $\hat{\boldsymbol{r}}$ denotes the orientation of a vector from the center of mass of molecule 1 to the center of mass of molecule 2 in a laboratory-frame coordinate system, $(\ldots|\ldots)$ denotes a Clebsch-Gordan coefficient, $Y_{\lambda m}$ is a spherical harmonic, and $\boldsymbol{R}_i$ is a vector indicating the bond length and direction of molecule i in the frame of reference where the Z axis is along a laboratory-fixed direction. Alexander and DePristo truncated the sum in Eq. (1) to 6 terms, namely those with $(\lambda_1\lambda_2\lambda)$ equal to (000), (112), (011), (123), (101), and (213). The coefficients $U^e_{\lambda_1\lambda_2\lambda}$ for the fifth and sixth terms are equal by symmetry to minus those for the third and fourth.

To use the Alexander-DePristo potential for the present calculations we had to add a vibrational dependence. This was done by extending an approximation of Gianturco et al [8] for the vibrational dependence of the short-range repulsive

[1] The V-V transition probabilities in [4] and [5] are systematically low by a few per cent due to an error in some of the vibrational matrix elements. There are two additional corrections to [5]: on p. 187, the number of operations per step should be $34\frac{2}{3}N^3$, which, when combined with our actual execution time for the $N = 948$ run, yields a lower bound for the execution rate of 139 MFLOPS

interactions and by using accurate R_i-dependent multipole moments to simulate the vibrational dependence of long-range electrostatic interactions.

For the short-range vibrational dependence, we follow Gianturco et al who wrote [8]

$$U_{\lambda_1\lambda_2\lambda} = U^e_{\lambda_1\lambda_2\lambda}(r)\exp[-\alpha_{\lambda_1\lambda_2\lambda}(R_1+R_2-2R_e)], \tag{3}$$

where R_e is the classical equilibrium internuclear distance of HF and

$$\alpha_{\lambda_1\lambda_2\lambda} = -[U^e_{\lambda_1\lambda_2\lambda}(r_0)]^{-1}\left.\frac{dU^e_{\lambda_1\lambda_2\lambda}}{dr}\right|_{r=r_0}. \tag{4}$$

They originally suggested this for $(\lambda_1\lambda_2\lambda)=(000)$, but we employ it here for all $(\lambda_1\lambda_2\lambda)$. Gianturco et al also suggested that r_0 be the translational classical turning point. We set r_0 equal to 4.1 a_0 because that is approximately the largest distance close to a typical classical translational turning point for which none of the $U^e_{\lambda_1\lambda_2\lambda}$ are passing through zero or are near to a local extremum.

The vibrational dependence of the long-range potential may be added more accurately. In the Alexander-DePristo potential the coefficients U^e_{112} and U^e_{123} take the form

$$U^e_{112} = -c_1e^{-c_2r} - c_3e^{-c_4r} - (2/15)^{1/2}\mu^2r^{-3} \tag{5}$$

$$U^e_{123} = -(c_5/r - c_6)e^{-c_7r} + (1/7)^{1/2}\mu\theta r^{-4}, \tag{6}$$

where the c_i are constants, and μ and θ are the dipole and quadrupole moments, which were set equal to vibrationally averaged values of 0.716 and 1.93 a.u., respectively. First we replace μ^2 by $\mu(R_1)\mu(R_2)$ and $\mu\theta$ by $\mu(R_1)\theta(R_2)$, and then we replace the multipole moments in these expressions with the linear functions

$$\mu(R_i) = \mu_e + \beta_{\lambda_1\lambda_2\lambda}(R_i - R_e) \tag{7}$$

and

$$\theta(R_i) = \theta_e + \gamma_{\lambda_1\lambda_2\lambda}(R_i - R_e), \tag{8}$$

where μ_e and θ_e are values corresponding to the equilibrium internuclear separation [9, 10] and the $\beta_{\lambda_1\lambda_2\lambda}$ and $\gamma_{\lambda_1\lambda_2\lambda}$ are constants. The constants β_{112}, β_{123}, and γ_{123} were chosen so that $(d/dR_i)\exp(-\alpha_{\lambda_1\lambda_2\lambda}R_i)\mu(R_i)$ and $(d/dR_i)\exp(-\alpha_{\lambda_1\lambda_2\lambda}R_i)\theta(R_i)$ reproduce the experimental value of $d\mu/dR_i = 0.3169$ a.u. [9] and the theoretical value of $d\theta/dR_i = 1.601$ a.u. [11], respectively. Notice that U_{123} involves $\mu(R_1)\theta(R_2)$, but U_{213} involves $\theta(R_1)\mu(R_2)$.

The full potential is the sum of the interaction potential just described plus the potentials for the noninteracting diatoms. The latter are taken from the work of Murrell and Sorbie [12]. The resulting potential energy surface is called the modified Alexander-DePristo (MAD) surface.

To use the MAD potential for the scattering calculations we re-express it in a body-frame coordinate system as [13, 14]

$$\mathcal{V} = \sum_{q_1q_2\mu} v_{q_1q_2\mu}(r, R_1, R_2)\mathcal{Y}_{q_1q_2\mu}(\hat{r}_1, \hat{r}_2), \tag{9}$$

where

$$\mathcal{Y}_{q_1 q_2 \mu}(\hat{\boldsymbol{r}}_1, \hat{\boldsymbol{r}}_2) = \frac{4\pi}{[2(1+\delta_{\mu 0})]^{1/2}} [\, Y_{q_1 \mu}(\hat{\boldsymbol{r}}_1) Y_{q_2 - \mu}(\hat{\boldsymbol{r}}_2) + Y_{q_1 - \mu}(\hat{\boldsymbol{r}}_1) Y_{q_2 \mu}(\hat{\boldsymbol{r}}_2)], \quad (10)$$

in which the $v_{q_1 q_2 \mu}$ are linear combinations of the $U_{\lambda_1 \lambda_2 \lambda}$, and $\hat{\boldsymbol{r}}_1$ and $\hat{\boldsymbol{r}}_2$ are unit vectors along the molecular axes in the frame in which the vector connecting the molecular centers of mass defines the z axis. We note that although the MAD potential has only 6 terms in the laboratory-frame expansion (1), it gives rise to 9 terms in the body-frame expansion (9) that is used for calculating matrix elements in the vibrational-rotational basis. Six of these are shown in Fig. 1, for $R_1 = R_2 = 1.733\ a_0$, and the other three are related to three of those shown by symmetry.

The MAD potential is compared to the more accurate Redmon-Binkley [15] potential in a previous paper [5]. That comparison indicates that the approximation of Eqs. (3) and (4) does not seem to predict the character of the vibrational force equally validly for different orientations of approach. Yet the extent of rotational participation in V-V energy transfer may depend sensitively on the orientational dependence of the vibrational force. Further dynamics calculations with more accurate interaction potentials may be required to learn the effect of this approximation on the state-to-state transition probabilities. Nevertheless, even though the vibrational forces of the MAD potential are not quantitatively accurate, it provides a reasonable but simple test potential for which converged V-V energy transfer calculations may be used as a benchmark, and so we proceeded to carry out such calculations.

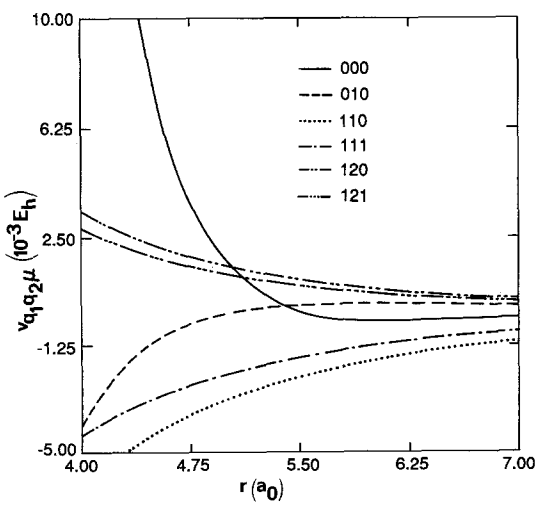

Fig. 1. Body-frame expansion coefficients $v_{q_1 q_2 \mu}(r, R_1 = 1.733 a_0, R_2 = 1.733 a_0)$ as a function of r for the MAD potential. The legend in the upper right identifies the triads of q_1, q_2, and μ. The units are millihartrees ($10^{-3}\ E_h$) and bohrs (a_0)

3. Scattering calculations

3.1. Theoretical formulation

The close coupling approximation for the quantum mechanical wave function for nuclear motion is

$$\psi_{n_0} = \frac{1}{r} \sum_{n=1}^{N} X_n(\boldsymbol{x}, \hat{\boldsymbol{r}}) f_{nn_0}(r, E), \tag{11}$$

where $\boldsymbol{x}$ denotes the collection of $\hat{\boldsymbol{r}}$, $\boldsymbol{R}_1$, and $\boldsymbol{R}_2$, E denotes the total energy, X_n is a symmetrized basis function, f_{nn_0} is a radial translational wave function, and n and n_0 are channel indices. Equation (11) leads to N coupled ordinary differential equations, the close coupling equations, for the f_{nn_0} [16–21] and these are solved by the R matrix propagation method [22–24] with the usual reactance-matrix boundary conditions. The state-to-state transition probabilities are computed from the solutions, and they converge to the accurate solution of the nuclear-motion Schroedinger equation as the basis becomes complete, i.e., as $N \to \infty$ in (11).

The basis functions we use are eigenfunctions of the total angular momentum, the molecule interchange operator, and the parity operator; this block diagonalizes the potential matrix in the total angular momentum quantum number J, its component M on a laboratory-fixed axis, the interchange symmetry quantum number η, and the parity quantum number P, and thus it allows the close coupling equations to be solved separately for each J, η, and P (the solutions are independent of M). The index n in (11) then specifies a set of quantum numbers (v_1, v_2), (j_1, j_2), j_{12}, l, J, M, η, and P, where v_1 and v_2 are vibrational quantum numbers, j_1 and j_2 are rotational quantum numbers, and j_{12} is the quantum number for the vector sum of the rotational angular momenta of the two molecules. Because it is not possible to distinguish which molecule has which set of quantum numbers, only sets with $v_1 > v_2$ or with $v_1 = v_2$ and $j_1 \geq j_2$ are included. We only consider the initial state $v_1 = v_2 = 1$, $j_2 = j_2 = 0$, $J = 0$. This state has even interchange symmetry, and it is only coupled to other basis functions that are also symmetric under this operation; thus we restrict our basis to such symmetric functions. In addition, this initial state has even parity so we only need basis functions with $P = +1$. Although they are not independent quantum numbers it is convenient to define v_{sum} as $v_1 + v_2$ and j_{sum} as $j_1 + j_2$. To select the basis functions for a given calculation we choose a maximum value $v_{\text{sum,max}}$ for v_{sum}; and for each $v_{\text{sum}} \leq v_{\text{sum,max}}$ we choose a maximum value $j_{\text{sum,max}}(v_{\text{sum}})$ for j_{sum}. In summary then, we include all possible combinations of (v_1, v_2), (j_1, j_2), j_{12}, and l consistent with these conditions on $v_1 \geq v_2$ and on $j_1 \geq j_2$ and with $J = M = 0$, $\eta = P = +1$. As a consequence of the interchange symmetry, the physically meaningful transition probabilities are to symmetric final states that can be labelled either by $v_1 > v_2$ with any pair of j_1 and j_2 or by $v_1 = v_2$ with $j_1 \geq j_2$.

Further details of the calculations and the numerical algorithms are given in previous papers [3, 5].

The calculations yield transition probabilities $P_{v_1 j_1 v_2 j_2 \to v_1' j_1' v_2' j_2'}$. In the present article we concentrate on a single initial state, $(v_1 j_1 v_2 j_2) = (1010)$. In addition to these eight-index transition probabilities, which are already summed over l' and j_{12}', we also consider probabilities summed over subsets of final rotational states. We define the rotationally summed V-V transition probability as

$$P^{VV}_{j_{sum}'} = \sum_{\substack{j_1' j_2' \\ j_1'+j_2'=j_{sum}'}} P_{1010 \to 2 j_1' 0 j_2'} \tag{12}$$

and the total V-V transition probability as

$$P^{VV} = \sum_{j_{sum}'} P^{VV}_{j_{sum}'} \tag{13}$$

Similarly we define the rotationally summed V-T, R transition probability as the sum of the $P_{1010 \to 1 j_1' 0 j_2'}$ values. The V-V and V-T, R language is convenient (and conventional) but technically oversimplified—in the former case since the V-V process always includes a small translational component, and it also includes a rotational component except when $j_{sum}' = 0$, and in the latter case since we do not include the two-quantum process $(v_1' = v_2' = 0)$ in the V-T, R probabilities. The results show that, at least for the potential used here, the rotational component of the V-V process is not negligible, but the two-vibrational-quanta V-T, R de-excitation process is less likely than the one-quantum process by about two orders of magnitude.

3.2. Basis sets

We consider three values of the initial relative translational energy E_{rel}. For each energy we performed calculations with several basis sets. In particular, we use the same value of $j_{sum,max}$ for $v_{sum} \leq 2$, and smaller values for larger v_{sum}. The compositions of the basis sets are summarized in Table 1. Not all basis functions correspond to open (i.e., energetically accessible) channels; the number of open channels for each basis set and energy is summarized in Table 2.

Table 1. Basis sets for *V–V* energy transfer calculations

	$j_{sum,max}$				
Basis	$v_{sum} \leq 2$	$v_{sum} = 3$	$v_{sum} = 4$	$v_{sum} = 5$	N
1	8	6	...	...	400
2	9	7	...	...	530
3	10	8	...	...	694
4	11	9	...	...	880
5	10	8	8	...	824
6	10	8	8	1	948

Table 2. Number of open channels represented in the basis at each relative translational energy (in meV)

Basis	2.455	29	76
1	162	184	239
2	207	229	284
3, 5, 6	264	286	341
4	327	349	404

4. Results

4.1. V-V *energy transfer*

First we consider the process

$$\mathrm{HF}(v_1=1, j_1=0)+\mathrm{HF}(v_2=1, j_2=0) \rightarrow \mathrm{HF}(v_1'=2, j_1')+\mathrm{HF}(v_2'=0, j_2').$$

Table 3 summarizes the convergence of the rotationally summed and total V-V transition probabilities with respect to increasing the number of basis functions. First consider the calculations with $j_{\mathrm{sum,max}}=8$, 9, 10, and 11 for $v_{\mathrm{sum}} \leq 2$ and $j_{\mathrm{sum,max}}=6$, 7, 8, and 9, respectively, for $v_{\mathrm{sum}}=3$, excluding channels with $v_{\mathrm{sum}}>3$. These calculations involved 400, 530, 694, and 880 channels, respectively. Comparison of the 880-channel calculations to the 694-channel calculations show convergence of P^{VV} to better than 1% at all the energies considered here. In Table 3, 10 of the 12 probabilities for the 694-channel and 880-channel calculations agree to within 0.004, and the discrepancies are 0.005 and 0.014 for the other

Table 3. Partially summed transition probabilities $P_{j_{\mathrm{sum}}'}^{\mathrm{VV}}$

E_{rel} (meV)	Open channels	Basis	N	Open-channel basis functions	P_0^{VV}	P_1^{VV}	P_2^{VV}	P_3^{VV}	P^{VV}
2.455	1548	1	400	162	0.711	0.039	0.061	0.024	0.844
		2	530	207	0.809	0.035	0.014	0.003	0.861
		3	684	264	0.846	0.035	0.002	0.002	0.885
		4	880	327	0.846	0.034	0.006	0.007	0.893
		5	824	264	0.891	0.037	0.003	0.003	0.933
		6	948	264	0.897	0.038	0.003	0.003	0.940
29	1671	1	400	184	0.882	0.039	0.010	0.004	0.936
		2	530	229	0.914	0.039	0.002	0.005	0.960
		3	694	286	0.919	0.042	0.007	0.006	0.976
		4	880	349	0.915	0.043	0.010	0.008	0.978
		5	824	286	0.933	0.041	0.010	0.005	0.990
		6	948	286	0.931	0.040	0.012	0.006	0.990
76	1888	1	400	239	0.899	0.049	0.012	0.006	0.968
		2	530	284	0.850	0.050	0.044	0.006	0.951
		3	694	341	0.809	0.047	0.063	0.008	0.930
		4	880	404	0.795	0.049	0.065	0.009	0.921
		5	824	341	0.748	0.035	0.082	0.009	0.878
		6	948	341	0.730	0.032	0.089	0.010	0.866

two probabilities. This comparison demonstrates that the rotational basis of basis set 3 is well converged for $v_{sum} \leq 3$. It is interesting to note that the convergence is attained at $j_{sum,max} = 10$ for these V–V calculations, whereas rigid rotator calculations [5] for the Alexander–DePristo potential require $j_{sum,max}$ values of about 12–14 in order to converge the results. Next we consider calculations that employ the converged rotational basis of basis set 3 for $v_{sum} \leq 3$ and also include channels with $v_{sum} > 3$ in order to converge the vibrational basis. Two additional basis sets were considered, one, with 824 channels, which has $j_{sum,max} = 6$ for $v_{sum} = 4$ and no states with $v_{sum} \geq 5$, and another, our largest basis of 948 channels, in which we included basis functions with $j_{sum} = 7$ and 8 for $v_{sum} = 4$ and those with $j_{sum} = 0$ and 1 for $v_{sum} = 4$ and 5. Values of $P^{VV}_{j_{sum}}$ and P^{VV} calculated with these basis sets are also given in Table 3. Comparison of the 824-channel calculations to the 948-channel calculations shows convergence of P^{VV} to better than 1.4% at all three energies. If we also consider $P^{VV}_{j_{sum}}$, we see that for 9 of the 12 probabilities in Table 5, the 824-channel and 948-channel calculations differ by 0.003 or less and for the other probabilities the discrepancies are 0.006, 0.007, and 0.019. The convergence is considered acceptable, especially at the two lower energies. Furthermore since the comparison of bases 3 and 4 shows that $j_{sum,max} = 8$ is sufficient for the $v_{sum} = 3$ channels, it should also be sufficient for $v_{sum} = 4$. The final values of the well converged rotationally summed V–V transition probabilities are summarized in Table 4.

The state-to-state V–V transition probabilities $P_{1010 \to 2j'_1 0 j'_2}$ for $j'_{sum} \leq 2$ as calculated with the four largest basis sets are given in Table 5. As for the results in Table 3, if basis 3 agrees with basis 4 and basis 5 with basis 6, then basis 6 should be considered converged. For the most part, probabilities with both $j'_1 \leq 1$ and $j'_2 \leq 1$ are well converged. The final values of the well converged state-to-state transition probabilities are summarized in Table 6.

4.2. V–R, T *energy transfer*

Next we consider the processes

$$HF(v_1 = 1, j_1 = 0) + HF(v_2 = 1, j_2 = 0) \to HF(v'_1 = 1 \text{ or } 0, j'_1) + HF(v'_2 = 0, j'_2).$$

Selected transition probabilities from the two largest calculations (bases 4 and 6) are compared in Table 7, and we see that although convergence is not obtained for these probabilities (the calculations differ from each other in $v_{sum,max}$ and in all six $j_{sum,max}$ limits), the probabilities are very small. Nevertheless the V–R, T results are worth considering here because of the interesting contrast of the j'_{sum} distributions for the V–V and V–R, T processes. Examination of these distributions

Table 4. Partially summed transition probabilities

E_{rel} (meV)	P^{VV}_0	P^{VV}_1	P^{VV}_2	P^{VV}
2.455	0.90	0.038	0.003	0.94
29	0.93	0.040	0.012	0.99

Table 5. State-to-state transition probabilities $P_{1010\to 2j_1'0j_2'}$

j_1'	j_2'	ΔE[a]	Basis	2.455[b]	29[b]	76[b]
0	0	21	3	0.85	0.92	0.81
			4	0.85	0.92	0.79
			5	0.89	0.93	0.75
			6	0.90	0.93	0.73
1	0	17	3	0.029	0.033	0.023
			4	0.028	0.036	0.025
			5	0.030	0.029	0.017
			6	0.031	0.028	0.015
0	1	16	3	0.006	0.010	0.024
			4	0.006	0.007	0.024
			5	0.007	0.012	0.018
			6	0.007	0.012	0.017
1	1	12	3	0.0003	0.006	0.062
			4	0.0017	0.009	0.064
			5	0.0003	0.009	0.081
			6	0.0004	0.011	0.089
2	0	7	3	0.0020	0.0010	0.0005
			4	0.0038	0.0009	0.0006
			5	0.0020	0.0010	0.0005
			6	0.0021	0.0010	0.0005
0	2	6	3	0.0002	0.0002	0.0002
			4	0.0005	0.0004	0.0003
			5	0.0003	0.0003	0.0003
			6	0.0003	0.0003	0.0003

[a] Transitional energy defect in meV (21 meV = 172 cm^{-1})
[b] E_{rel} in meV (76 meV = 613 cm^{-1})

for the V-R, T probabilities shows that vibrational de-excitation is often accompanied by 3-10 quanta of rotational excitation. Comparison to Table 2 or 3 shows that there is a much larger rotational component to the vibrational de-excitation than to the V-V energy transfer for the MAD potential. Thus the small rotational component of the V-V energy transfer process cannot be interpreted simply as a lack of rotational-vibrational coupling in the surface.

Finally we note that the unconverged transition probabilities for de-excitation

Table 6. State-to-state transition probabilities

j_1'	j_2'	2.455[a]	29[a]
0	0	0.90	0.93
1	0	0.03	0.03
0	1	0.007	0.01
1	1	0.0004	0.011
2	0	0.002	0.001

[a] E_{rel} in meV

Table 7. Selected transition probabilities for vibrational de-excitation

				$E_{rel} = 2.455$ meV		$E_{rel} = 29$ meV		$E_{rel} = 76$ meV	
v_1'	j_1'	v_2'	j_2'	$N = 880$	$N = 948$	$N = 880$	$N = 948$	$N = 880$	$N = 948$
1	4	0	3	2.4 (−4)	1.9 (−5)	2.3 (−4)	2.3 (−5)	1.6 (−4)	7.9 (−5)
1	4	0	4	3.7 (−5)	1.0 (−4)	5.8 (−5)	1.5 (−4)	9.2 (−5)	2.2 (−4)
0	4	0	3	5.7 (−8)	7.6 (−7)	9.7 (−8)	1.6 (−6)	2.4 (−7)	3.5 (−6)
0	4	0	4	1.6 (−7)	1.6 (−7)	1.0 (−7)	2.7 (−7)	7.4 (−7)	8.7 (−7)

by a single vibrational quantum are one-to-three orders of magnitude larger than those for two-quantum de-excitation.

5. Computational considerations

The close coupling calculations were performed using a code specially vectorized for the Control Data Corporation Cyber 205 pipeline vector computer. We used single precision (64-bit) arithmetic and the Minnesota Supercomputer Center's two-pipe Cyber 205. The largest calculation, for three energies with 948 channels, required about 17.5 hours of computer time. It is interesting to estimate how much time would be required to carry out this calculation on a Digital Equipment Corporation VAX 11/780 with scalar floating point accelerator. In our initial tests [3], we compared times on such a VAX to those on the Cyber 205 for a test case having $N = 101$. Additional tests of the matrix routines on the VAX indicate that for $N > 50$, the time for a calculation on the VAX scales with N as $N^{3.0}$. Using this factor to scale the execution time for a full calculation with $N = 101$, we estimate for a full three-energy calculation with $N = 948$ a time of 3.0×10^4 hours (3.4 years). Thus we estimate a speed enhancement of the Cyber 205 over the VAX of about a factor of 1700. The speed enhancements of the vector pipeline Cyber 205 relative to the scalar VAX would increase with increasing N since the number of scalar operations increases as N^3 whereas we found that, for $N =$ 400–948, the CPU time on the Cyber 205 was still increasing only proportionally to $N^{2.6}$. We estimate speed in millions of floating point operations per second (MFLOPS) as follows. Most of time (about 95% for the $N = 948$ run and about 92–94% for other N for this potential) used for our calculations is spent on matrix manipulations; in particular for each propagation step at the first energy we must diagonalize an $N \times N$ matrix, multiply three $N \times N$ matrices, and solve two sets of linear equations for N different unknown vectors, while for each step for the second and third energies we must perform two $N \times N$ matrix multiplications and solve a set of linear equations for N different unknown vectors. The number of arithmetic operations (addition or multiplication) to perform various matrix steps is analyzed elsewhere [5, 25]; in particular the number to perform a matrix multiplication is $2N^3$, the number to perform a linear equation solution is $8N^3/3$, and we will take the number to perform a matrix diagonalization to be $10N^3$ (which may be a slight, 5–10%, underestimate for our problem), so that the number of operations will be about $34\frac{2}{3}N^3$ per step, which, when combined

with the number of propagation steps we used, 297, and with our actual execution time for the $N = 948$ run, 17.5 CPU hours, yields a lower bound for the operation rate of 139 MFLOPS. This compares favorably to the maximum theoretically obtainable value [26] of 200 MFLOPS on a two-pipeline machine running in single precision performing linked triads.

6. Discussion and conclusions

We have shown that it is possible to use currently available vector pipeline computers to solve very large sets of close coupling equations and that it is possible to converge three-dimensional calculations of V–V energy transfer for diatom–diatom collisions, even though a very large number of channels are required. Although the present calculations, being restricted to zero total angular momentum, cannot be compared to experiment, they provide benchmarks for testing approximate dynamical theories that can more easily be applied to all total angular momenta.

Table 5 shows that the state-to-state V–V energy transfer cross sections peak at a final state that is nonresonant by 21 meV, and the transition probabilities to other channels with smaller translational energy defects are smaller by factors of thirty or more. It would be interesting to learn the sensitivity of this rotational distribution to the nature of the potential. It would also be interesting to use these results to test whether semiclassical methods, which are more easily applied than the close coupling method to V–V energy transfer problems, would yield similar values of the total V–V transition probability and the accompanying rotational distribution if they are applied using the same potential as used here.

In future work we plan to study the dependence of the results on the nature of the intermolecular potential. This requires more effort for calculating matrix elements of the potential, and it may require even larger numbers of channels. It is encouraging for the latter reasons to see that pipeline computers can be applied with near peak efficiency to solve the close coupling equations for this kind of problem.

Acknowledgments. This work was supported in part by the University of Minnesota Supercomputer Institute, by the National Science Foundation under grants nos. CHE83-17944 and CHE86-17063 and by the Control Data Corporation through the PACER Fellowship program.

References

1. Kondratiev VV, Nikitin EE (1981) Gas-phase reactions, chap 4. Springer, Berlin Heidelberg New York
2. Yardley JT (1980) Introduction to molecular energy transfer, chap. 5 Academic Press, New York
3. Schwenke DW, Truhlar DG (1985) In: Numrich RW (ed) Supercomputer applications. Plenum Press, New York, p 295
4. Schwenke DW, Truhlar DG (1986) Theor Chim Acta 69:175
5. Schwenke DW, Truhlar DG (1986) In: Dupuis M (ed) Supercomputer simulations in chemistry. Springer, Berlin, Heidelberg New York, p 165
6. Alexander MH, DePristo AE (1976) J Chem Phys 65:5009

7. Yarkony DR, O'Neil SV, Schaefer HF III, Baskin CP, Bender CF (1974) J Chem Phys 60:855
8. Gianturco FA, Lamanna UT, Battaglia F (1981) Int J Quantum Chem 19:217
9. Sileo RN, Cool TA (1976) J Chem Phys 65:117
10. Huber KD, Herzberg G (1979) Constants for diatomic molecules. Van Nostrand, Princeton
11. Maillard D, Silvi B (1980) Mol Phys 40:933
12. Murrell JN, Sorbie KS (1974) J Chem Soc Faraday Trans II 70:1552
13. Gioumousis G, Curtiss CF (1961) J Math Phys 2:96
14. Launay JM (1977) J Phys B 10:3665
15. Redmon MJ, Binkley JS J Chem Phys, in press
16. Arthurs AM, Dalgarno A (1960) Proc Roy Soc London A 256:540
17. Davison WD (1962) Faraday Discuss Chem Soc 33:71
18. Green S (1975) J Chem Phys 62:2271
19. Rabitz H (1976) In: Miller WH (ed) Dynamics of molecular collisions, part A. Plenum Press, New York, p 33
20. Alexander MH, DePristo AE (1977) J Chem Phys 66:2166
21. Secrest D (1979) In: Bernstein RB (ed) Atom-molecule collision theory. Plenum Press, New York, p 377
22. Light JC, Walker RB (1976) J Chem Phys 65 4272
23. Truhlar DG, Mullaney NA (1978) J Chem Phys 68:1574
24. Truhlar DG, Harvey NM, Onda K, Brandt MA (1979) In: Thomas L (ed) Algorithms and computer codes for atomic and molecular quantum scattering theory, vol 1. National Resource for Computation in Chemistry, Lawrence Berkeley Laboratory, Berkeley, CA, p 220
25. Golub GH, Van Loan CF (1983) Matrix computations. Johns Hopkins University Press, Baltimore, pp 53, 69, 282
26. Hockney RW, Jesshope CF (1981) Parallel computers. Adam Hilger, Bristol, p 124